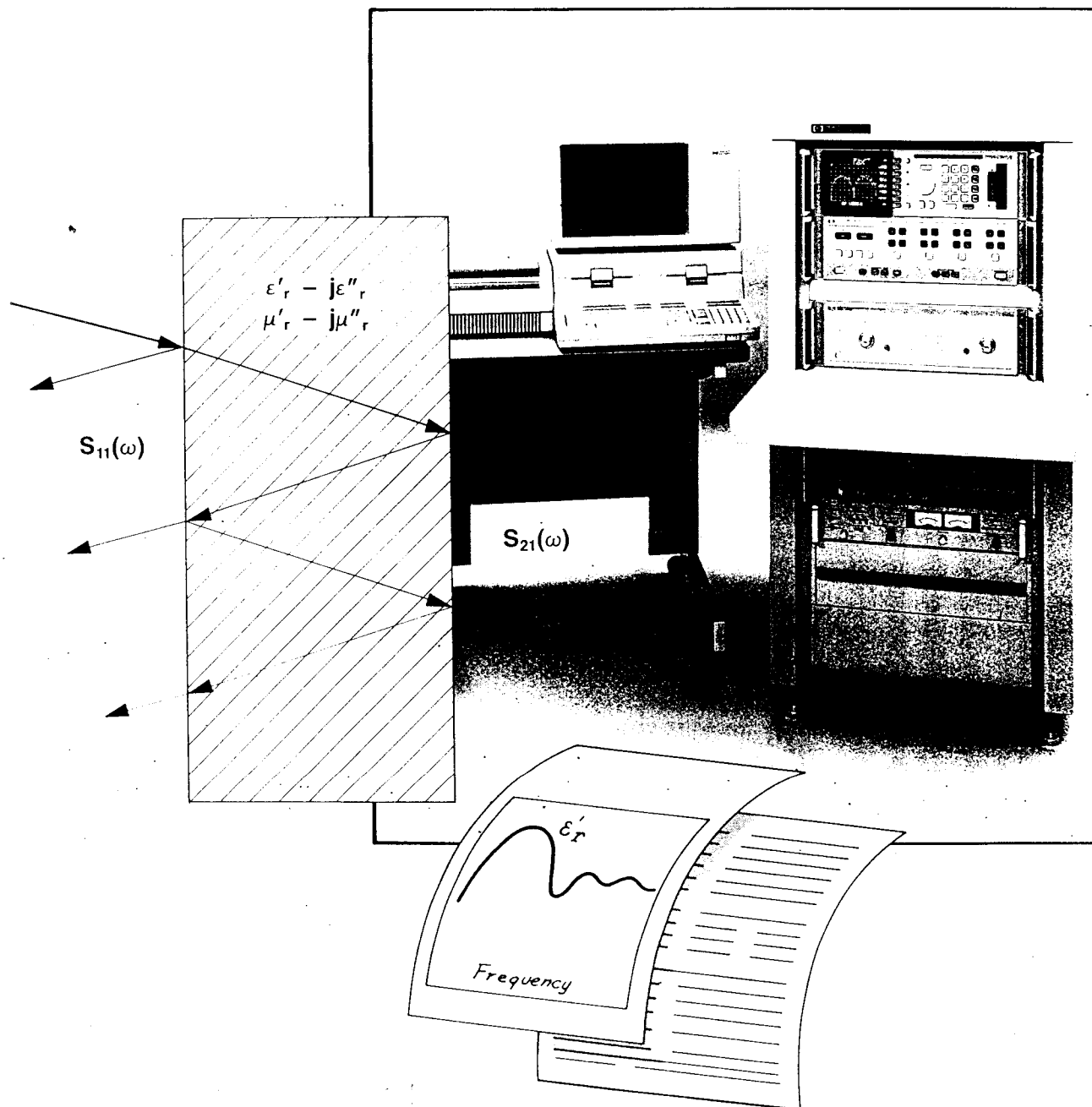


*Measuring Dielectric Constant  
with the HP 8510 Network Analyzer*

*The Measurement of Both Permittivity  
and Permeability of Solid Materials*



## Introduction

Measurement of complex permittivity ( $\epsilon_r$ ) and permeability ( $\mu_r$ ), both vector quantities of dielectric or absorptive materials, has gained increasing importance with expanding use of the RF and microwave spectrum, particularly in communications and electromagnetic countermeasure applications. In addition, the network analyzer has seen increasing use in non-destructive measurements to determine the chemical composition of a sample dielectric material. The method described here is suited for the measurement of complex permittivity and permeability of solid type materials which have both dielectric and metallic characteristics, and with a relatively high loss tand. For low loss tand materials, the basic measurement principle also gives valid results for the dielectric constant ( $\epsilon_r$ ) measurement, but the measurement uncertainty of loss factor ( $\epsilon''_r$ ) is high.

These measurements have been made for years using numerous methods. A conventional technique involves a two-step process using a slotted line or network analyzer. First, the sample is backed up by a short circuit and the input impedance is measured. Next, the short circuit is moved  $\frac{1}{4} \lambda$  from the sample to simulate an open circuit termination (where  $\lambda$  is the incident signal wavelength), and a second measurement is made. The results of these two measurements are used to solve simultaneous equations for  $\epsilon_r$  and  $\mu_r$ . This procedure is repeated for each frequency of interest. Uncertainties in the measurement include test set-up frequency response, mismatch, and directivity errors, as well as the uncertainty in the physical position of the short circuit.

Despite the fact that the measurements are difficult to make, time consuming, and prone to errors, much data has been gathered using this or similar methods.

This note describes a procedure for using the HP 8510 network analyzer system with simple-to-fabricate test fixtures, with the capability to simultaneously measure both  $\epsilon_r$  and  $\mu_r$  at up to 401 frequency points with high speed, and enhanced accuracy. Also, the time domain gating capability of the HP 8510 can eliminate residual mismatch errors from the measurement data to improve accuracy even further.

## Basic Theory

The original idea for computation of complex permittivity and permeability from S-parameter data was suggested by Nicolson and Ross<sup>1</sup> for their time domain measurement of dielectric materials. In the ideal case, consider the sample material installed in 50-ohm ( $Z_0$ ) air line as shown in Figure 1.

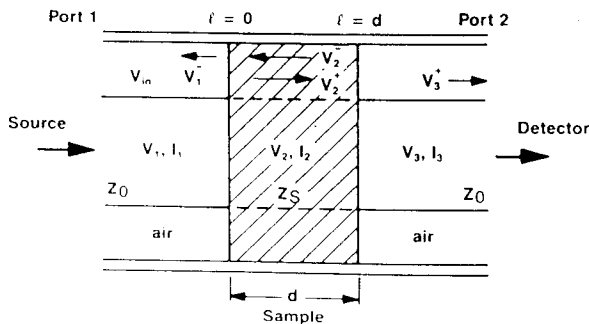


Figure 1. Air Line with Filled Material.

Assuming no source and load mismatches, then equations [A1] through [A4] in the Appendix describe the electromagnetic relationships in each region of Figure 1. By solving the boundary conditions at  $l = 0$  and  $l = d$ , it is possible to relate  $S_{11}(\omega)$  and  $S_{21}(\omega)$  to the reflection coefficient ( $\Gamma$ ) and transmission coefficient ( $T$ ) with the following equations:

$$\begin{aligned} S_{11}(\omega) &= \frac{(1 - T^2) \Gamma}{1 - T^2 \Gamma^2} \\ S_{21}(\omega) &= \frac{(1 - \Gamma^2) T}{1 - T^2 \Gamma^2} \end{aligned} \quad [1]$$

Where  $\Gamma$  is the reflection coefficient between  $Z_0$  and  $Z_s$  when the length of materials is infinite ( $l = \infty$ ); and

$$\Gamma = \frac{Z_s - Z_0}{Z_s + Z_0} = \frac{\sqrt{\frac{\mu_r}{\epsilon_r}} - 1}{\sqrt{\frac{\mu_r}{\epsilon_r}} + 1} \quad [2]$$

The term  $T$  is the transmission coefficient in the materials (of finite length) and can be written:

$$T = \exp(-j\omega \sqrt{\mu_r \epsilon_r} \cdot d) = \exp[-j(\omega/c) \sqrt{\mu_r \epsilon_r} \cdot d] \quad [3]$$

Equation [1] allows  $\Gamma$  and  $T$  to be derived by measuring  $S_{11}(\omega)$  and  $S_{21}(\omega)$ . These quantities can then be used to calculate the complex permittivity ( $\epsilon_r$ ) and permeability ( $\mu_r$ ).

## Measurement System

Network analyzers measure the magnitude and phase response of linear networks and components by comparing the incident signal with the signal transmitted by the device or reflected from its input. S-parameters are used to express measurement results because they provide a simple notation to represent the device responses with exact data consisting of a linear magnitude ratio and relative phase angle. Also, the S-parameters may be used to compute other quantities such as SWR, complex impedance, and group delay, as well as complex permittivity and permeability.

Figure 2 shows a signal flowgraph using S-parameter notation for a two-port device. The notation is read  $S_{out in}$  where the first number represents the output port and the second number represents the input port. Thus,  $S_{11}(\omega)$  is the response measured at port 1 with the stimulus applied at port 1. The notation  $S_{11}(\omega)$  represents the frequency domain response characteristic.

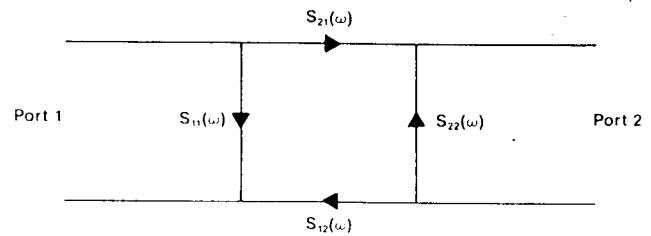


Figure 2. S-Parameter Flowgraph Notation.

As shown in Figure 3, signal separation devices separate the stimulus signal from the source into an incident signal sent to the device under test and a reference signal against which the magnitude and phase of the reflected and transmitted signals from the sample under test are compared. These signals are processed by the network analyzer to develop the complex ratios for display.

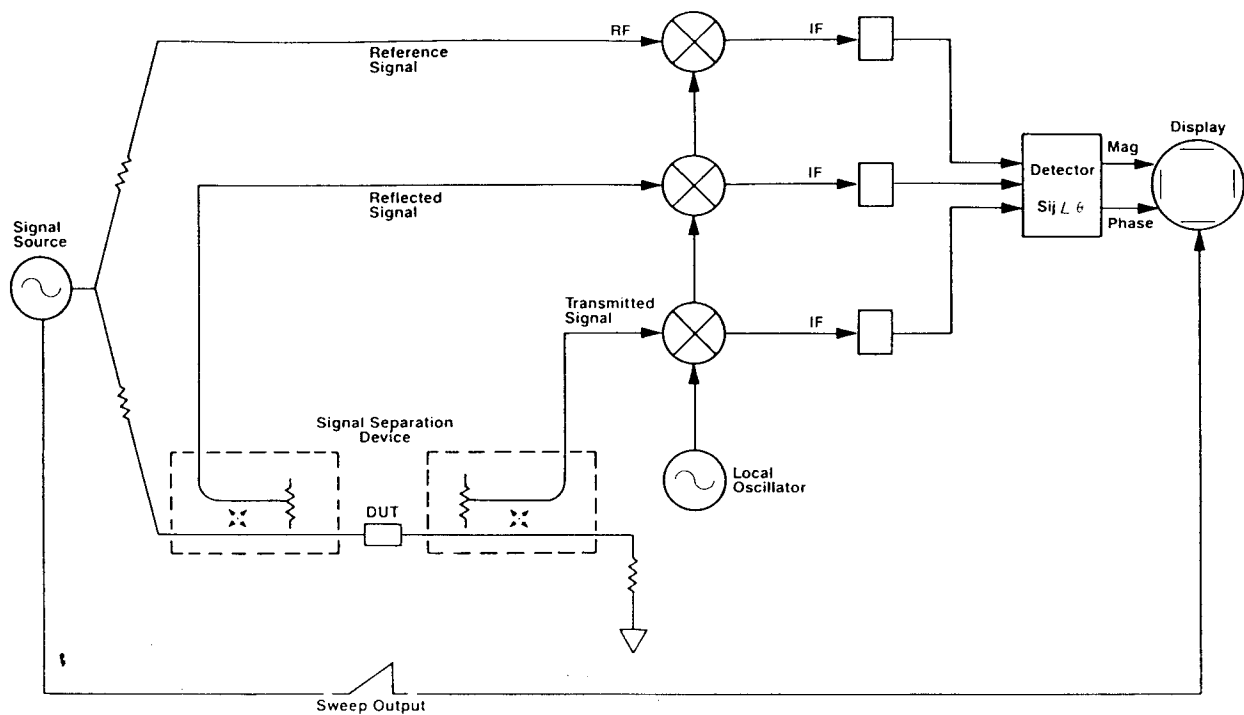


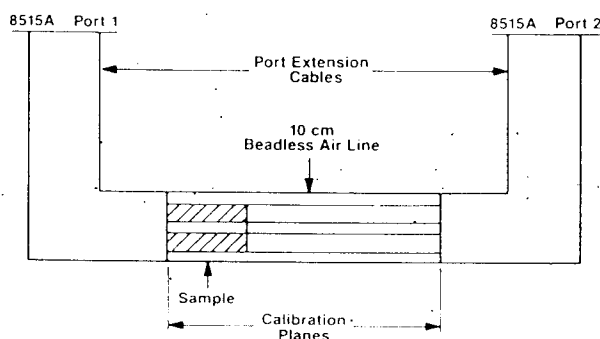
Figure 3. Network Analyzer Simplified Block Diagram.

## Measurement Fixtures

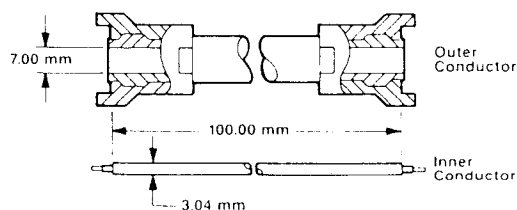
To measure the complex permittivity and permeability with the HP 8510 network analyzer, a measurement fixture must be fabricated to hold the sample. This sample holder is a coaxial or waveguide transmission line, and a dielectric sample must be machined to slide into the sample holder. It is from the S-parameters of this transmission line that  $\epsilon_r$  and  $\mu_r$  are calculated. Any 50-ohm coaxial beadless air line or waveguide

can be used as a sample holder. However, it is recommended that the length of the sample holder is the same as that of the sample to minimize the effect of the loss and phase shift in the transmission line between the sample and measurement reference planes. (The optimum length of the sample material is discussed later.) For the measurements described here, two different types of sample holders are used. Figure 4 shows the physical dimensions of the coaxial and waveguide sample holders.

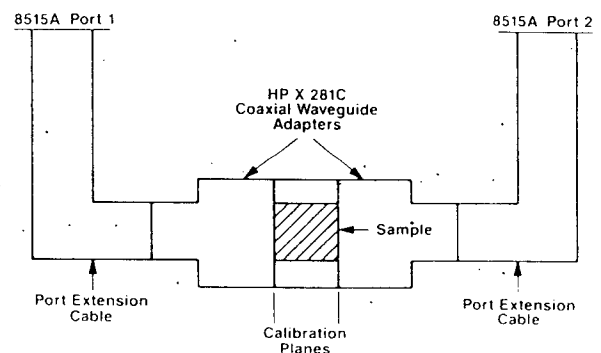
### Coaxial Measurement Setup



### Coaxial Sample Holder (10 cm APC-7 Beadless Air Line)



### Waveguide Measurement Setup



### Waveguide Sample Holder (X band)

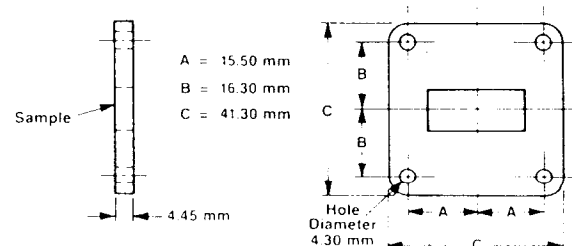


Figure 4. Coaxial and Waveguide Sample Holders.

The coaxial sample holder used here consists of a 50-ohm, 7 mm beadless air line (10 cm) with the sample material formed to replace the air dielectric at one end of the air line. Using this fixture, it is important that the sample completely fills the area between inner and outer conductor, and presents a flat surface at the reference plane. Measurement calibration is performed using the standards in the HP 85050A 7 mm Calibration Kit.

For these measurements, a waveguide sample holder was fabricated by cutting the flange from a length of standard waveguide of the appropriate band (X-band). It is important that the end surfaces of the flange are as flat and smooth as possible so that good mating contact is achieved. Measurement calibration used typical waveguide standards: a fixed or sliding  $Z_0$  termination, a  $\lambda_{gm}/8$  offset short, and a  $3\lambda_{gm}/8$  offset short (where  $\lambda_{gm}$  is the waveguide wavelength at the geometric mean frequency).

The waveguide sample holder has the advantage that the rectangular shape makes the sample easy to form. However, the frequency coverage is restricted by the high pass characteristic of the waveguide. The coaxial fixture provides wide frequency coverage, although it is much more difficult to form the sample into the appropriate shape so that the sample completely fills the area between the inner and outer conductor in the beadless air line structure.

## Measurement Procedure

The following measurements are made with the HP 8510 network analyzer system which consists of the HP 8510A network analyzer, the HP 8340A synthesized sweeper, the HP 8515A S-parameter test set and an HP Model 9000 Series 200 computer. Since best accuracy and repeatability are required for the measurement of  $S_{11}(\omega)$  and  $S_{21}(\omega)$ , the full 2-port calibration with step sweep mode and averaging is used.

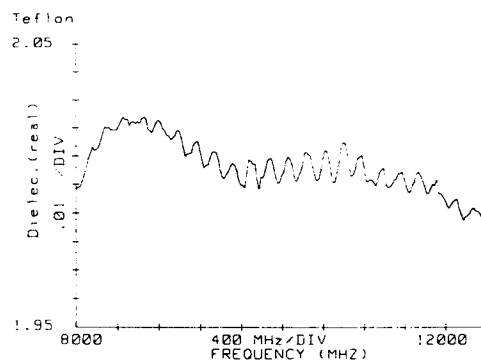
Conversion from S-parameter data measured by the HP 8510A to the dielectric properties is accomplished by reading trace data into the computer, performing the required conversions, and then plotting or listing the results (Refer to Appendix B for the measurement flow chart). Since  $T$  in equations [A8] and [A11] is a complex number, these equations have an infinite number of roots (i.e., the imaginary part of the logarithm is equal to the angle of the complex value plus  $2\pi n$ , where  $n$  is equal to the integer of  $d/\lambda_g$ , and  $\lambda_g$  is the actual wavelength in the material). However, the correct value of  $n$  can be decided by analysis of the group delay.<sup>2</sup> Also, the reference plane rotation in the waveguide can be performed by using an external computer as described in Appendix D.

## Measurement Results

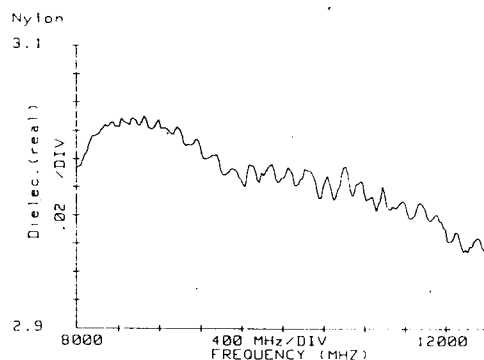
Three different materials, Teflon®, nylon, and polyiron, were measured both in coaxial and waveguide sample holders. The length of each sample in the waveguide fixture is 0.445 cm and measured at 23°C. Figure 5 shows the measurement results of each material in the X-band waveguide sample fixture. The measured data agrees well with the data measured using other techniques. For example, the measured  $\epsilon'_r$  for Teflon was 2.01 at 11.7 GHz and this is very close to the value 2.043 which was quoted by K. Kobayashi using resonator techniques.<sup>3</sup> As Teflon is a nonmagnetic material, its  $\mu'_r$  should be unity. The measured value was 1.00 at 11.7 GHz.

In the case of nylon, using the coaxial sample holder, the measured  $\epsilon'_r$  at 3 GHz was 2.99 which agrees well with the value 3.03 which was quoted by Von Hippel.<sup>4</sup> Again, as nylon is nonmagnetic material, its relative permeability should be unity. The measured  $\mu'_r$  value was 1.02 at 3 GHz. Although no data are available for comparison at higher frequencies, the measured values at 10 GHz using the waveguide sample holder were 3.03 for  $\epsilon'_r$  and 1.00 for  $\mu'_r$ , which compares well with the lower frequency data.

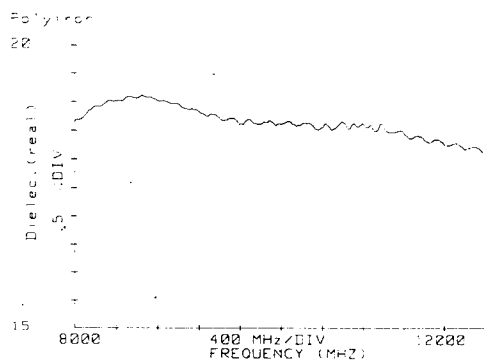
As an example of a metallic device, a polyiron sample (a mixture of epoxy and iron) was measured. Since polyiron is metallic, the relative permeability is greater than 1 and also it shows relatively high loss dielectric constant and permeability (i.e., relatively large  $\epsilon''_r$  and  $\mu''_r$ ).



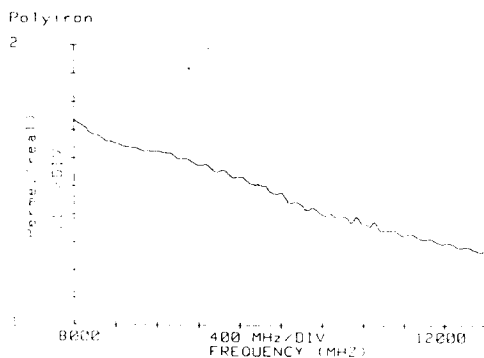
a.  $\epsilon'_r$  for Teflon



b.  $\epsilon'_r$  for Nylon



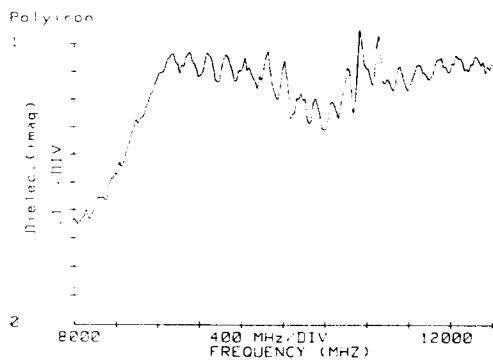
c.  $\epsilon'_r$  for Polyiron



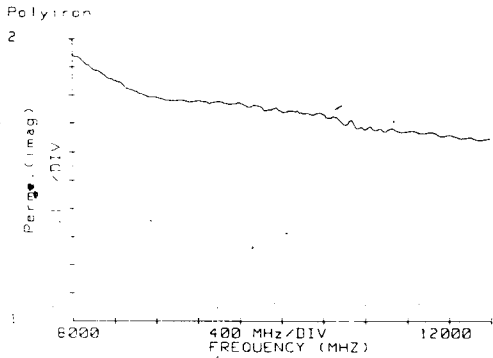
d.  $\mu'_r$  for Polyiron

Figure 5. The Characteristics of  $\epsilon$ , and  $\mu$ , for Teflon, Nylon and Polyiron (' denotes the real part, " denotes the imaginary).

Teflon® is a US registered trademark of the Dupont Corporation.



e.  $\epsilon_r''$  for Polyiron



f.  $\mu_r''$  for Polyiron

Figure 5. (Continued) The Characteristics of  $\epsilon_r$  and  $\mu_r$  for Teflon, Nylon and Polyiron [ $'$  denotes the real part;  $''$  denotes the imaginary].

Table 1 shows the  $\epsilon_r$  and  $\mu_r$  characteristic of Teflon measured in the coaxial air line (10 cm). The length of sample is 0.5 cm and measured at 2 GHz to 4 GHz, and 23°C.

Frequency (MHz)	Permittivity		Permeability	
	Real	Imaginary	Real	Imaginary
2000	2.05	0.026	1.02	0.018
2100	2.05	0.025	1.01	0.016
2200	2.05	0.027	1.02	0.016
2300	2.05	0.024	1.02	0.017
2400	2.04	0.023	1.02	0.018
2500	2.04	0.021	1.02	0.020
2600	2.04	0.019	1.02	0.022
2700	2.05	0.017	1.02	0.021
2800	2.05	0.017	1.02	0.023
2900	2.06	0.022	1.02	0.028
3000	2.05	0.017	1.01	0.021
3100	2.05	0.021	1.01	0.017
3200	2.05	0.023	1.01	0.016
3300	2.05	0.027	1.01	0.011
3400	2.04	0.027	1.01	0.011
3500	2.04	0.030	1.01	0.009
3600	2.04	0.026	1.02	0.013
3700	2.03	0.024	1.02	0.013
3800	2.03	0.019	1.02	0.018
3900	2.03	0.017	1.02	0.019
4000	2.03	0.012	1.01	0.023

Table 1. Teflon Measurement in Coaxial Fixture.

## Measurement Speed

The data included here was measured using the full 2-port error model, which requires actual measurement of all four S-parameters of the two-port sample holder, at 201 frequency points, using the step sweep mode with an averaging factor of 128. After measurement calibration, the system requires about 2 minutes to produce fully averaged data and perform the required conversions. Measurement time can be reduced by reducing the number of frequency points to 51 or 101 and decreasing the averaging factor.

## Accuracy Considerations

Several error factors, such as instrumentation, dimensional errors caused by an air gap between material and conductors, by roughness of the surface of the material, and by the higher order modes excitation, must be considered in this measurement. Due to the complexity of modeling these contributors, only the instrumentation and dimensional errors are considered.

**Instrumentation Error.** The measurement errors,  $\Delta\epsilon_r$  and  $\Delta\mu_r$ , due to instrumentation error can, in principle, be calculated by using the partial derivative technique. However, the following error analysis is done using a computer simulation. Because the instrumentation error of the HP 8510A depends on the magnitude of the measured  $S_{11}(\omega)$  and  $S_{21}(\omega)$ , it is necessary to know the behavior of these parameters for the given material as a function of frequency.

The characteristics of  $S_{11}(\omega)$  and  $S_{21}(\omega)$  for the given material can be calculated from equations [1], [A12], and [A13]. Figure 6 shows the simulated characteristics of the Teflon sample (length = 0.445 cm) in the X-band waveguide sample fixture. The assumptions are:  $\epsilon_r' = 2.03$ ,  $\epsilon_r'' = 0.0008$ ,  $\mu_r' = 1$ , and  $\mu_r'' = 0$  at those frequencies.

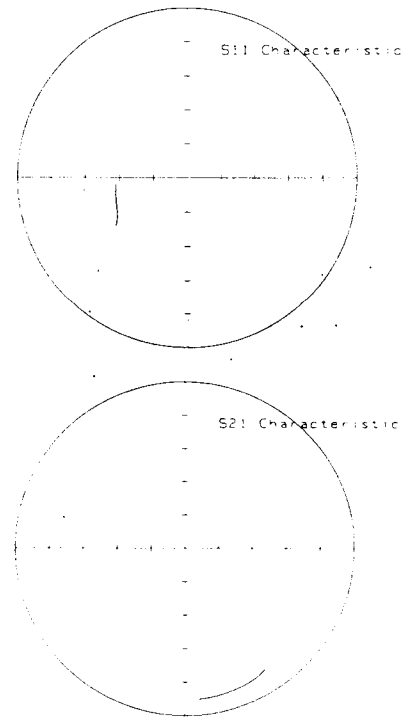


Figure 6. Simulated  $S_{11}(\omega)$  and  $S_{21}(\omega)$  for Teflon.

(8-12 GHz, Full Scale = 1)

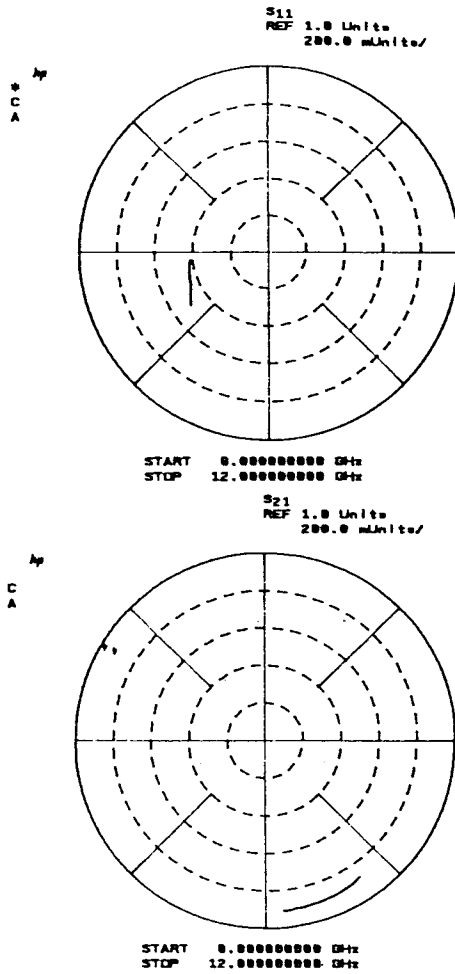


Figure 7. Measured  $S_{11}(\omega)$  and  $S_{21}(\omega)$  for Teflon.  
(8-12 GHz, Full Scale = 1)

Figure 7 shows the actual measured data and shows that the simulations agree with the measurement.

The magnitudes of  $S_{11}(\omega)$  and  $S_{21}(\omega)$  vary from 0.507 to 0.422 and 0.861 to 0.906, respectively. The instrumentation errors of the HP 8510 system for  $S_{11}(\omega)$  and  $S_{21}(\omega)$  for this magnitude range are about  $\pm 0.005$  ( $\pm 1$  degree), and  $\pm 0.005$  ( $\pm 0.25$  degree), respectively.

After knowing the calculated  $S_{11}(\omega)$  and  $S_{21}(\omega)$ , the measurement error for  $\epsilon_r$  and  $\mu_r$  can be calculated. The computed maximum measurement errors,  $\Delta\epsilon_r$  and  $\Delta\mu_r$ , for this measurement are:  $\Delta\epsilon_r = \pm 0.02$ ;  $\Delta\mu_r = \pm 0.03$ ;  $\Delta\epsilon''_r = \pm 0.02$ ; and  $\Delta\mu''_r = \pm 0.03$ . The measured  $\epsilon_r$  and  $\mu_r$  for Teflon are within this measurement uncertainty. From the computer simulations, the measurement accuracy for  $\epsilon_r$  and  $\mu_r$  with this technique was found to be approximately  $\pm 1\%$  when the permittivity or permeability of the sample is relatively small, as with Teflon and nylon. However, because of the large errors in  $\epsilon''_r$  and  $\mu''_r$ , low loss  $\tan\delta$  measurements are difficult with this technique. To get reasonable accuracy, the loss  $\tan\delta$  of the sample should be greater than 0.1.

**Optimum Length of Sample Material.** The instrumentation error for the HP 8510 system depends on the magnitudes of  $S_{11}(\omega)$  and  $S_{21}(\omega)$ . The magnitude and phase errors for  $S_{11}(\omega)$  increase when  $|S_{11}(\omega)|$  approaches 0 and decrease when approaching 1. The magnitude and phase errors for  $S_{21}(\omega)$  are about  $\pm 0.05$  dB and  $\pm 0.25$  degrees, respectively, and these are practically independent of the magnitude of  $S_{21}(\omega)$  when  $|S_{21}(\omega)|$  is between 0.1 to 1. For further information on the instrumentation error, please refer to the HP 8510 data sheet.

As  $|S_{21}(\omega)|$  is usually bigger than 0.1, the minimum error for  $\epsilon_r$  and  $\mu_r$  occurs when  $|S_{11}(\omega)|$  is maximum. Because of the  $(2n+1)\lambda_g/4$  transformer effects the maximum and minimum  $|S_{11}(\omega)|$  occur when the length is  $(2n+1)\lambda_g/4$  and  $(2n+1)\lambda_g/2$ , respectively. This means that if the sample length is selected to be length  $= \lambda_g/4$ , the uncertainties for  $\epsilon_r$  and  $\mu_r$  will be minimized.

The wavelength  $\lambda_g$  in the sample material in the coaxial sample fixture can be calculated by the following equation:

$$\lambda_g = \text{Re} \left( \frac{\lambda_0}{\sqrt{\epsilon_r \cdot \mu_r}} \right) \quad [4]$$

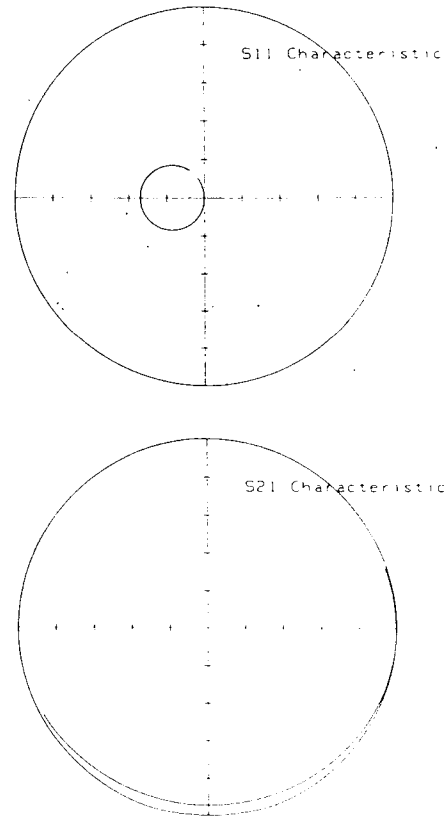
where  $\lambda_0$  is the wavelength in free space.

Because of the dispersive characteristic of the waveguide sample fixture, the  $S_{11}(\omega)$  and  $S_{21}(\omega)$  characteristics differ from that of the coaxial sample fixture. In the waveguide, the wavelength  $\lambda_g$  can be calculated as follows:

$$\lambda_g = \text{Re} \left( \frac{1}{\sqrt{\left( \frac{\epsilon_r \mu_r}{\lambda_0^2} - \frac{1}{\lambda_c^2} \right)}} \right) \quad [5]$$

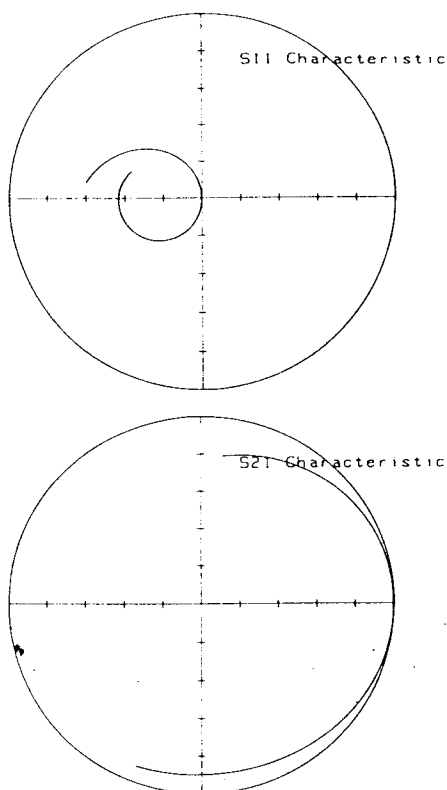
(In coaxial line,  $\lambda_c = \infty$ )

Figure 8 shows the simulated  $S_{11}(\omega)$  and  $S_{21}(\omega)$  responses (from 8 to 12 GHz) of the Teflon sample (2.5 cm length) when measured in the coaxial and waveguide sample holders, and it indicates how the behavior of the two responses differs between the two measurements.



A. In Coaxial Sample Holder (Full Scale = 1)

Figure 8. Simulated Teflon  $S_{11}(\omega)$  and  $S_{21}(\omega)$  behavior (8-12 GHz; length = 2.5 cm;  $\epsilon'_r = 2.03$ ;  $\epsilon''_r = 0.0008$ ,  $\mu'_r = 1$ ;  $\mu''_r = 0$ )



B. In Waveguide Sample Holder (Full Scale = 1)

Figure 8. (Continued) Simulated Teflon  $S_{11}(\omega)$  and  $S_{21}(\omega)$  behavior (8-12 GHz; length = 2.5 cm;  $\epsilon'_r = 2.03$ ;  $\epsilon''_r = 0.0008$ ,  $\mu'_r = 1$ ;  $\mu''_r = 0$ ).

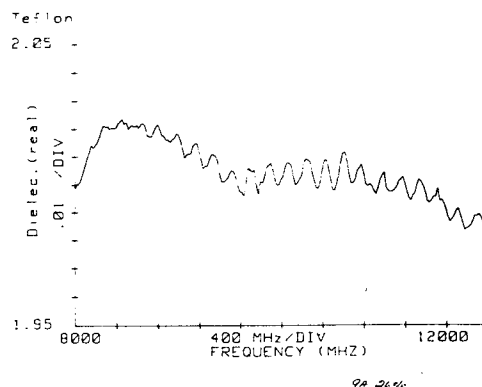
**Uncertainty of the Sample Length.** The uncertainty for  $\epsilon_r$  and  $\mu_r$  caused by a small error in specifying the actual physical length of the sample material is, for practical purposes, proportional to the percentage of the error. Experience indicates this to be true for length specification errors smaller than 5 percent. Thus, a 1 percent error in the length of material produces about 1 percent error in the  $\epsilon_r$  and  $\mu_r$  data. As it is not unusually difficult to form the sample length to within  $\pm 0.01$  mm accuracy, the uncertainty due to an error in the length characteristic of the sample material is not a main factor for this measurement method.

## Further Enhancements Using Gating

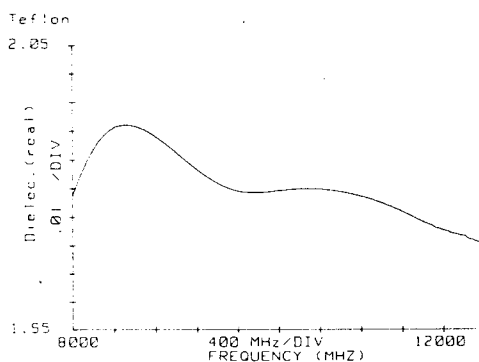
Because of imperfect system source and load match, and because accuracy enhancement techniques cannot completely remove these mismatch effects from the measurement, residual mismatch errors will be seen in the measured data. As the effective load match of the HP 8510 system after full 2-port error correction is about 40 dB (0.01), the mismatch error is  $\pm 0.005$  when the reflection coefficient magnitude of the material is 0.5. This will cause some ripple in the  $S_{21}(\omega)$  characteristic and produce visible ripple in the  $\epsilon_r$  and  $\mu_r$  characteristics. This error appears as noise in the time domain response. By gating around the main path  $S_{21}$  response of the

sample, the effects of the mismatch error can be further reduced. This improvement also takes place in the (gated) frequency domain  $S_{21}(\omega)$  data and subsequently in the  $\epsilon_r$  and  $\mu_r$  data. For further information on time domain and gating, please refer to the HP 8510 Operating and Programming Manual.

Figure 9 shows the  $\epsilon_r$  characteristic of Teflon with and without time domain gating. Gating has reduced the effects of source and load match ripple in the  $\epsilon_r$  characteristic.



A. No Time Domain Gating.



B. With Time Domain Gating (gate width 2 ns).

Figure 9.  $\epsilon_r$  of Teflon With and Without Time Domain Gating.

## Conclusion

This technique is usable for the measurement of both  $\epsilon_r$  and  $\mu_r$  of materials which have relatively high loss  $\tan\delta$  ( $>0.1$ ), and it is especially useful for the evaluation of absorptive materials. The measurement of low loss  $\tan\delta$  samples ( $<0.01$ ), however, is difficult using this technique and requires a different one, such as the resonator techniques.<sup>5</sup>

## Appendix A

The following shows the derivation of the formulas for permittivity and permeability.

$$\begin{aligned} V_1 &= V_1^+ e^{-j\gamma_0 \ell} + V_1^- e^{j\gamma_0 \ell} \\ I_1 &= \frac{1}{Z_0} (V_1^+ e^{-j\gamma_0 \ell} - V_1^- e^{j\gamma_0 \ell}) \end{aligned} \quad \ell \leq 0 \quad [A1]$$

$$\begin{aligned} V_2 &= V_2^+ e^{-j\gamma_1 \ell} + V_2^- e^{j\gamma_1 \ell} \\ I_2 &= \frac{1}{Z_S} (V_2^+ e^{-j\gamma_1 \ell} - V_2^- e^{j\gamma_1 \ell}) \end{aligned} \quad 0 \leq \ell \leq d \quad [A2]$$

$$\begin{aligned} V_3 &= V_3^+ e^{-j\gamma_0 (\ell-d)} \\ I_3 &= \frac{1}{Z_0} (V_3^+ e^{-j\gamma_0 (\ell-d)}) \end{aligned} \quad \ell \geq d \quad [A3]$$

where,

- $\gamma_0$  (Propagation constant in free space) =  $\omega \sqrt{\mu_0 \cdot \epsilon_0}$
- $\gamma_1$  (Propagation constant in material) =  $\omega/c \sqrt{\mu_r \cdot \epsilon_r}$
- $\omega$  = Angular frequency
- $c$  = Velocity of light in free space
- $\mu_0$  = Permeability of free space
- $\epsilon_0$  = Permittivity of free space
- $\mu_r$  = Relative permeability of material
- $\epsilon_r$  = Relative permittivity of material
- $d$  = Length of material
- $Z_0$  = Intrinsic impedance in air line
- $Z_d$  = Intrinsic impedance in material

The boundary conditions for Figure A1 are:

$$\begin{aligned} V_1 &= V_2 \quad \text{at} \quad \ell=0 \\ I_1 &= I_2 \quad \text{at} \quad \ell=0 \\ V_2 &= V_3 \quad \text{at} \quad \ell=d \\ I_2 &= I_3 \quad \text{at} \quad \ell=d \end{aligned} \quad [A4]$$

From equations [A1] through [A4], the  $\Gamma$  and  $T$  can be written:

$$\Gamma = K \pm \sqrt{K^2 - 1} \quad [A5]$$

where,

$$K = \frac{\{S_{11}^2(\omega) - S_{21}^2(\omega)\} + 1}{2S_{11}(\omega)}$$

$$T = \frac{\{S_{11}(\omega) + S_{21}(\omega)\} - \Gamma}{1 - \{S_{11}(\omega) + S_{21}(\omega)\}\Gamma} \quad [A6]$$

From equation [2], [3] we can define  $x$  and  $y$  as follows:

$$\frac{\mu_r}{\epsilon_r} = \left( \frac{1 + \Gamma}{1 - \Gamma} \right)^2 = x \quad [A7]$$

$$\mu_r \cdot \epsilon_r = - \left\{ \frac{c}{\omega d} \ln \left( \frac{1}{T} \right) \right\}^2 = y \quad [A8]$$

then,

$$\mu_r = \sqrt{\frac{x \cdot y}{x}} \quad [A9]$$

$$\epsilon_r = \sqrt{\frac{y}{x}} \quad [A10]$$

For measurements using the waveguide sample holder, the equations [A7] and [A8] can be written as follows:<sup>2</sup>

$$\frac{1}{\Lambda^2} = \left( \frac{\epsilon_r \cdot \mu_r}{\lambda_0^2} - \frac{1}{\lambda_c^2} \right) = - \left[ \frac{1}{2\pi d} \ln \left( \frac{1}{T} \right) \right]^2 \quad [A11]$$

where,

$$\text{Re} \left( \frac{1}{\Lambda} \right) = \frac{1}{\lambda_g}$$

$$\mu_r = \frac{1 + \Gamma}{\Lambda (1 - \Gamma)} \cdot \frac{1}{\frac{1}{\lambda_0^2} - \frac{1}{\lambda_c^2}} \quad [A12]$$

where  $\lambda_0$  = free space wavelength,  $\lambda_c$  = cutoff wavelength of the waveguide and,

$$\epsilon_r = \frac{\left( \frac{1}{\Lambda^2} + \frac{1}{\lambda_c^2} \right) \lambda_0^2}{\mu_r} \quad [A13]$$

Note: Equations [A12] and [A13] are also applicable to measurements using the coaxial sample holder, where  $\lambda_c = \infty$ .

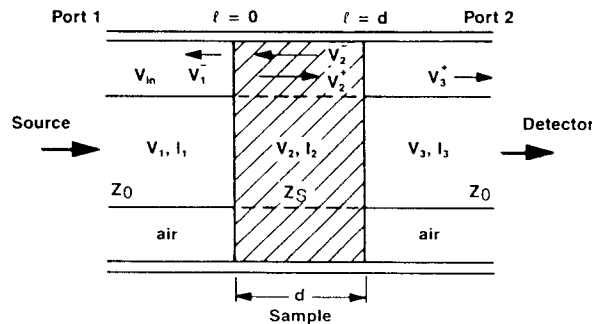


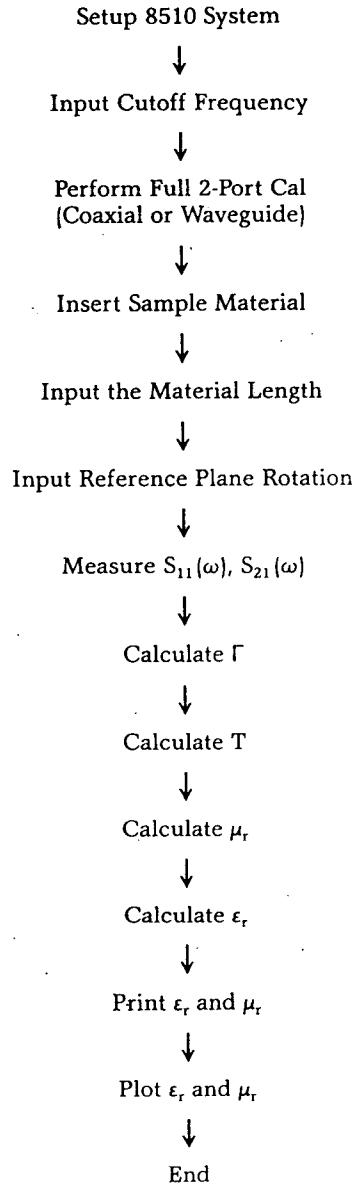
Figure A1. Air Line with Filled Material



## Appendix B

The following chart shows the measurement procedure for permittivity and permeability of solid type materials.

**The measurement procedure for  $\epsilon_r$  and  $\mu_r$  measurements.**



$$\Gamma = K \pm \sqrt{K^2 - 1}, \text{ where } K = \frac{[S_{11}^2(\omega) - S_{21}^2(\omega)] + 1}{2S_{11}(\omega)}$$

$$T = \frac{[S_{11}(\omega) + S_{21}(\omega)] - \Gamma}{1 - [S_{11}(\omega) + S_{21}(\omega)]\Gamma}$$

$$\mu_r = \frac{1 + \Gamma}{\Lambda(1 - \Gamma) \sqrt{\frac{1}{\lambda_0^2} - \frac{1}{\lambda_c^2}}}$$

$$\epsilon_r = \frac{\left(\frac{1}{\Lambda^2} + \frac{1}{\lambda_c^2}\right) \lambda_0^2}{\mu_r}$$

$$\text{where, } \frac{1}{\Lambda^2} = -\left[\frac{1}{2\pi d} \ln\left(\frac{1}{T}\right)\right]^2$$

## Appendix C

Following is an example calculation for a polyiron type material.

Measured  $S_{11}(\omega) = 0.552 \angle 178.8^\circ$

$S_{21}(\omega) = 0.305 \angle -156.1^\circ$

and the measurement frequency,  $f_0$ , is 10 GHz.

The sample is inserted into the X band sample holder. The length of sample is 0.2 cm, and the cutoff frequency for X band,  $f_c$ , is 6.557 GHz.

First calculate K.

$$K = \frac{[S_{11}^2(\omega) - S_{21}^2(\omega)] + 1}{2S_{11}(\omega)} = -1.126 + j 0.051$$

Therefore,

$$\begin{aligned} \Gamma &= K \pm \sqrt{K^2 - 1} \\ &= (-1.126 + j 0.051) \pm \sqrt{[1.1272 \angle 177.4^\circ]^2 - 1} \end{aligned}$$

Because  $|\Gamma| \leq 1$ , then,

$$\Gamma = (-1.126 + j 0.051) + (0.528 - j 0.109) = -0.598 - j 0.058$$

$$\begin{aligned} T &= \frac{[S_{11}(\omega) + S_{21}(\omega)] - \Gamma}{1 - [S_{11}(\omega) + S_{21}(\omega)]\Gamma} = -0.410 - j 0.201 \\ &= 0.457 \angle -153.9^\circ \end{aligned}$$

$$\begin{aligned} \ell n \left( \frac{1}{T} \right) &= \ell n (2.188 \angle 153.9^\circ) = \ell n (2.188 \angle 2.686 \text{ rad}) \\ &= \ell n (2.188) + j (2.686 + 2\pi n) \end{aligned}$$

where,  $n = 0, 1, 2, 3, \dots$ , the integer of  $(d/\lambda_g)$ . This  $n$  can be determined by analysis of the group delay,<sup>2</sup> or can be estimated from  $\lambda_g$  using the predicted values of  $\epsilon_r$  and  $\mu_r$  for the sample.

For the case that the parameter  $n$  is equal to 0, then,

$$\ell n \left( \frac{1}{T} \right) = 0.783 + j 2.686$$

Therefore,

$$\begin{aligned} \frac{1}{\Lambda^2} &= - \left[ \frac{1}{2\pi d} \ell n \left( \frac{1}{T} \right) \right]^2 = - \left[ \frac{1}{2\pi \times 0.2} (0.783 + j 2.686) \right]^2 \\ &= -4.960 \angle 147.4^\circ \end{aligned}$$

and,

$$\frac{1}{\Lambda} = \pm j 2.227 \angle 73.7^\circ$$

Because  $\text{Re} \left( \frac{1}{\Lambda} \right) \geq 0$ , then,

$$\frac{1}{\Lambda} = 2.137 - j 0.625 = 2.227 \angle -16.3^\circ$$

$$\frac{1 + \Gamma}{1 - \Gamma} = 0.249 - j 0.045 = 0.253 \angle -10.2^\circ$$

Since

$$f_0 = 10 \text{ GHz}, f_c = 6.557 \text{ GHz},$$

$$\lambda_0 = 3.0 \text{ cm}$$

$$\lambda_c = 4.575 \text{ cm}$$

Therefore,

$$\begin{aligned} \mu_r &= \frac{1 + \Gamma}{\Lambda (1 - \Gamma)} \sqrt{\frac{1}{\lambda_0^2} - \frac{1}{\lambda_c^2}} \\ &= \frac{2.227 \angle -16.3^\circ \times 0.253 \angle -10.2^\circ}{\sqrt{\frac{1}{3^2} - \frac{1}{4.575^2}}} = 2.242 \angle -26.5^\circ \end{aligned}$$

Thus,

$$\mu_r' = 2.0$$

$$\mu_r'' = 1.0$$

$$\epsilon_r = \frac{\left( \frac{1}{\Lambda^2} + \frac{1}{\lambda_c^2} \right) \lambda_0^2}{\mu_r}$$

$$= \frac{[-4.960 \angle 147.4^\circ + \frac{1}{4.575^2}] \times 3^2}{2.242 \angle -26.5^\circ} = 20.07 \angle -5.8^\circ$$

Thus,

$$\epsilon_r' = 20.0$$

$$\epsilon_r'' = 2.0$$

## Appendix D

### Reference plane rotation.

When the reference plane for the measurement is different from the original calibration plane, the corresponding phase shift must be removed from the measured  $S_{11}(\omega)$  and  $S_{21}(\omega)$  data. This will occur whenever the sample length is shorter than that of the sample holder. For measurements using the coaxial sample holder, this can be done by using the internal HP 8510A reference plane extension capability. However, for the waveguide sample holder, an external computer is required to remove the nonlinear phase shift caused by the dispersive characteristic. The phase shift for  $S_{11}(\omega)$  and  $S_{21}(\omega)$  can be calculated using the following equations.

For  $S_{11}(\omega)$ ,

$$\text{Phase shift} = \frac{360^\circ \times f_0}{c} \sqrt{1 - \left(\frac{f_c}{f_0}\right)^2} \times 2 \times a \quad A[14]$$

For  $S_{21}(\omega)$ ,

$$\text{Phase shift} = \frac{360^\circ \times f_0}{c} \sqrt{1 - \left(\frac{f_c}{f_0}\right)^2} \times (a + b) \quad A[15]$$

where,

$f_0$  = Measurement frequency.

$f_c$  = Cutoff frequency of the waveguide.

$f_c = 0$  for coaxial measurement.

$c$  = Velocity of light.

$a$  = Physical distance between the calibration plane and measurement plane of the port 1.

$b$  = Physical distance between the calibration plane and measurement plane of the port 2.

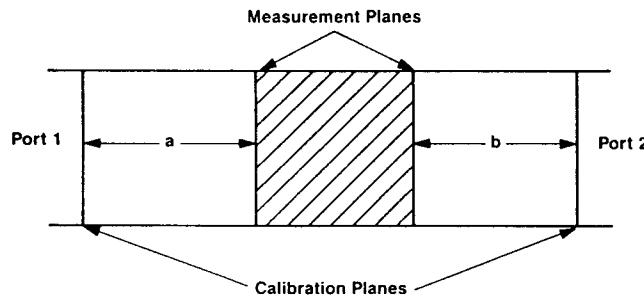


Figure A2. Reference Plane Rotation

## References

1. A.M. Nicolson, G.F. Ross. "Measurement of the Intrinsic Properties of Materials by Time Domain Techniques." IEEE Trans. Instrum. Meas., Vol. IM-19, pp. 377-382, Nov. 1970.
2. William B. Weir. "Automatic Measurement of Complex Dielectric Constant and Permeability at Microwave Frequencies." IEEE, Volume 62, No. 1, Jan., 1974.
3. Y. Kobayashi. "The Measurement of Complex Dielectric Constant at Microwave Frequencies." 1982, written in Japanese.
4. Arthur R. Von Hippel. "Dielectric Materials and Applications." The MIT Press, Cambridge, MA.
5. B.W. Hakki and P.D. Coleman. "A Dielectric Resonator Method of Measuring Inductive Capacities in the Millimeter Range." IRE Trans. Microwave Theory and Techniques, Vol. MTT-8, pp. 402-410, July, 1960.